EFDA–JET–CP(08)03-02

P. Buratti, C.D. Challis, M. Gryaznevich, T.C. Hender, E. Joffrin, T. Luce,
P. Smeulders and JET EFDA contributors

Radial Analysis of Beta-Limiting Modes in JET

“This document is intended for publication in the open literature. It is made available on the understanding that it may not be further circulated and extracts or references may not be published prior to publication of the original when applicable, or without the consent of the Publications Officer, EFDA, Culham Science Centre, Abingdon, Oxon, OX14 3DB, UK.”

“Enquiries about Copyright and reproduction should be addressed to the Publications Officer, EFDA, Culham Science Centre, Abingdon, Oxon, OX14 3DB, UK.”

Radial Analysis of Beta-Limiting Modes in JET

P. Buratti[1], C.D. Challis[2], M. Gryaznevich[2], T.C. Hender[2], E. Joffrin[3], T. Luce[4], P. Smeulders[1] and JET EFDA contributors*

JET-EFDA, Culham Science Centre, OX14 3DB, Abingdon, UK

[1]EURATOM-ENEA Fusion Association, C.R. Frascati, CP65, 00044 Frascati, Italy
[2]EURATOM-UKAEA Fusion Association, Culham Science Centre, OX14 3DB, Abingdon, OXON, UK
[3]Association EURATOM-CEA, DSM/DRFC, Cadarache, F-13108, France
[4]General Atomics, PO Box85608, San Diego, Ca92186-5608, USA
** See annex of M.L. Watkins et al, "Overview of JET Results ", (Proc. 21 st IAEA Fusion Energy Conference, Chengdu, China (2006)).*

Preprint of Paper to be submitted for publication in Proceedings of the
35th EPS Conference on Plasma Physics, Hersonissos, Crete, Greece
(9th June 2008 - 13th June 2008)

ABSTRACT.
Access to high β_N regimes with a q profile compatible with large bootstrap current has been systematically investigated in JET H-mode plasmas [1]. In these discharges with relatively broad pressure profile, the achievable β_N was limited by an n = 1 MHD instability that resulted in a soft but significant loss of confinement (Fig.1). Experiments have been performed with $q_{95} \approx 5$, as is envisaged for steady-state operation of ITER. β_N values in excess of 3 (Fig.1) have been achieved at q_{min} below 1.5, while at q_{min} close to 2 the beta-limiting mode occurred at lower values $\beta_N \approx 2$, as for the case shown in figures 2 and 3. The main features of the beta-limiting instability are:

- At $\beta_N \geq 2$ the mode has kink-like structure at first, and develops an m = 2 island after 100-200ms. Vice versa modes starting at $\beta_N < 2$ have an island from the beginning.
- Rotation frequency corresponding to plasma core toroidal rotation.
- Presence of low-amplitude precursors, often in the form of fishbones.
- Occurrence at β_N values above the threshold for resonant field amplification.

1. RADIAL ANALYSIS OF PHASE AND AMPLITUDE

The radial structure of the *n* = 1 mode has been investigated using 48 temperature channels with fast data acquisition from the Electron Cyclotron Emission (ECE) diagnostic. For each channel (k), the signal has been divided into a sequence of 4.6ms long data blocks and the cross-spectral density G_{kM} (f) with a reference magnetic signal (M) has been calculated dividing each block into N = 8 sub block samples and averaging. The phase angle of G_{kM} at the spectral peak corresponding to the mode frequency gives phase ϕ_k. Oscillation amplitude and coherence are given by $A_k = |G_{kM}|/\sqrt{G_{MM}}$ and $\gamma_{kM} = |G_{kM}|/\sqrt{G_{kk}G_{MM}}$ respectively. Expected random errors (absolute on ϕ_k and relative on A_k) are $\sqrt{1-\gamma_{kM}^2} = |\gamma_{kM}|/\sqrt{2N}$. Phase and amplitude profiles versus major radius coordinate (*R*) on the ECE sightline, with confidence intervals delimited by thin lines, are shown in figures 2(b) and 2(d). The phase profile is ideal-like in this time slice, i.e. it has no π-jumps that would reveal the presence of magnetic islands. Phase varies by 5.1 rad as *R* spans from 2.58 to 3.66m, due to the fact that the ECE sightline lies at $Z_0 \approx 17$cm below the magnetic axis plane, so that the poloidal angle varies with sightline coordinate as $\theta = \tan^{-1}(Z_0/(R-R_0))$. The phase profile is in rough agreement with the "baseline" expected for a mode with *m* = 2 poloidal number (black dashed curve in fig.2(d)).

The flux surface displacement (Fig.2(c)) has been estimated as $\xi = A\cos\theta/(dT_e/dR)$, where *A* is amplitude and the $\cos\theta$ factor estimates the actual T_e gradient from the derivative along the sightline coordinate. Results are only reliable for *R* > 3.2m, where a broad peak can be seen. Similar displacement profiles were observed for *n* = 1 modes in JET plasmas with Internal Transport Barriers (ITBs) and very peaked pressure profiles [3], but, while in ITB experiments the mode led to disruption at $\beta_N < 2$, in the high beta plasmas with moderate pressure peaking being described in this paper the mode typically saturated at displacement values below 5cm.

2. PHASE EVOLUTION AND ISLAND FORMATION

In this section the difference between measured phase and $m = 2$ baseline is considered. The latter is estimated by $\phi_2(R) = 2\theta(R) + \phi_0$, where ϕ_0 is an empirical shift accounting for the phase of the reference magnetic signal. Toroidal corrections (θ^* effect) are irrelevant since they give a constant phase shift along the ECE sightline. Shaping corrections are neglected. Figures 3a and 3b respectively show profiles at $t = 4.8$s (the same time-slice with ideal-like profile as in Fig.3) and at $t = 5.3$s. The latter features clear π-jumps (at $R = 2.6$ and 3.3m), which is the signature of the presence of an island. Full phase information is displayed in Fig.3(c), in which π-jumps appear as red-blue interfaces for $t > 4.87\,s$. Time evolution for three channels is shown in Fig.3(d). For a pure $m = 2$ mode the traces should lie on the dotted lines at 0 and $-\pi$,–as they actually do for t > 5s. The green trace, that represents the first channel on which the island appears, shows a progressive transition to $-\pi$ that deserves some discussion. As the mode character changes from kink-like to mixed kink-tearing, the growth of a magnetic island will superpose an odd (with respect to the $q = 2$ radius) $m = 2$ displacement to the pre-existing even one; some ECE channel close to the island will then detect a mixture of 0 and $-\pi$ oscillations within its spatial resolution; the result will be a decrease of signal amplitude, but the phase will be either 0 or $-\pi$. The actual result is different, in that the amplitude remains large while the phase changes progressively. This anomaly could be due either to a phase lag of the island with respect to the kink component (as expected for forced reconnection) or to overlap with different poloidal components ($m = 1$ or $m = 3$) that have even parity throughout. A mixture of different m components could also explain the slight deviation from $m = 2$ baseline (most evident in the red trace) that occurs when the mode is kink-like. The discharge considered in figure 3 had q_{min} close to 2 and the $n = 1$ mode developing at $\beta_N = 2.1$. The behaviour of discharges with lower q_{min} and higher β_N was quite similar, the only difference being a stronger deviation from the m=2 baseline in the kink-like stage. Different profiles, with one channel at $-\pi$ from the beginning, have been found in discharges with higher q_{min} and $n = 1$ mode appearing at β_N below 2; this could be due either to the prompt formation of a small island or to a radical change of mode structure from kink-like to double-tearing.

3. AMPLITUDE AND FREQUENCY EVOLUTION

The $m = 1$ mode appears first in the form of small “precursor” bursts, after which it grows and saturates in about 400ms. Figure 4(a) shows magnetic signal amplitude for a discharge at $\beta_N > 3$ (discharges at lower β_N tend to have smaller precursors but are generally similar to this). Clear mode growth starts at $t = 6.65\,s$; before this time precursors can be seen in between spikes due to edge localised modes. Rotation frequency is close to 12kHz for precursors and decreases to 9-10†kHz for the main mode (Fig.4(b)). In some discharges, including the one illustrated in Fig.3, a large-amplitude $q = 2$ fishbone appears before the growing mode; interestingly, its frequency span equals the frequency variation from precursors to growing mode; this indicates that precursors could be fishbones with small frequency span. Figure 4(c) shows toroidal rotation frequency contours

from charge exchange diagnostic and the position at which mode frequency matches toroidal rotation. Clearly the mode rotates at the same velocity as the plasma near midradius.

ACKNOWLEDGEMENT.

This work, supported by the European Communities under the EURATOM/ENEA contract of Association, was carried out within the framework of the European Fusion Development Agreement. The views and opinions expressed herein do not necessarily reflect those of the European Commission.

REFERENCES

[1]. C.D.Challis *et al.*, 34th EPS Conf. on Plasma Phys. ECA Vol 31F (2007) P5.124.

[2]. M.Gryaznevich *et al.*, invited paper at this Conference.

[3]. G.T.A. Huysmans et al., Nucl. Fusion **39** (1999) 1489.

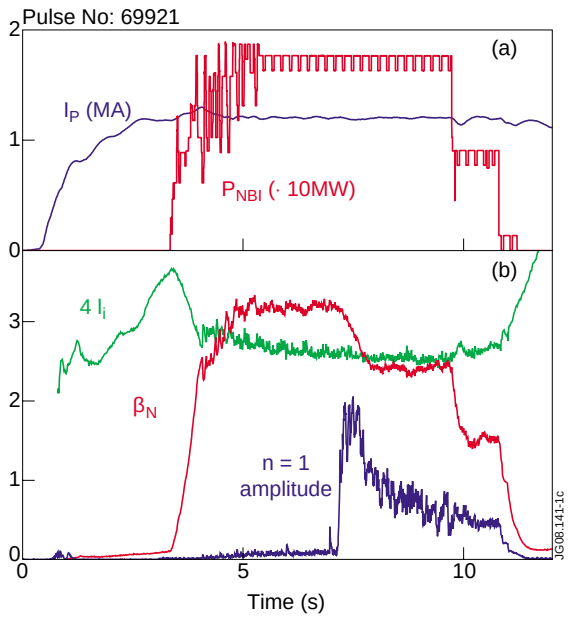

Figure 1: Time traces of (a) plasma current and heating power; (b) normalised beta, 4×internal inductance (as a rough estimate of ideal no-wall beta limit) and n=1 mode amplitude.

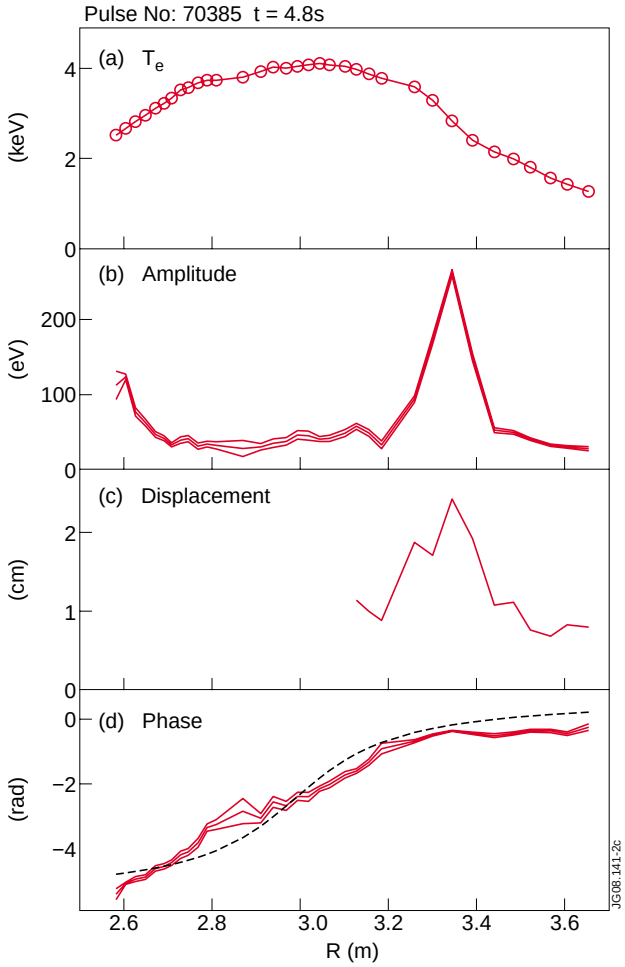

Figure 2: Profiles along the ECE sightline radial coordinate. (a) Mean T_e; (b) zero-to-peak oscillation amplitude; (c) displacement; (d) phase. Dashed line is expected phase for m=2.

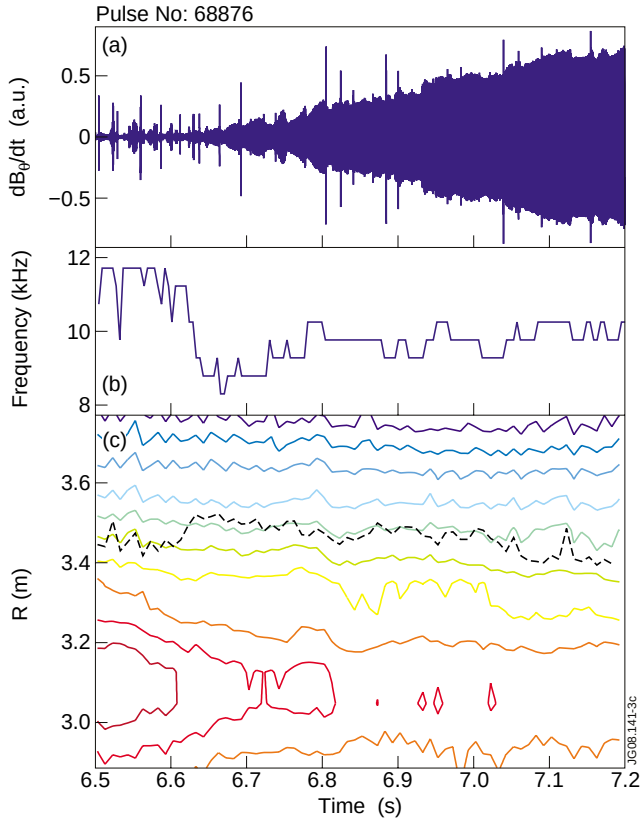

Figure 3: Phase evolution at the n=1 mode frequency (9 kHz) with m=2 phase baseline subtracted.

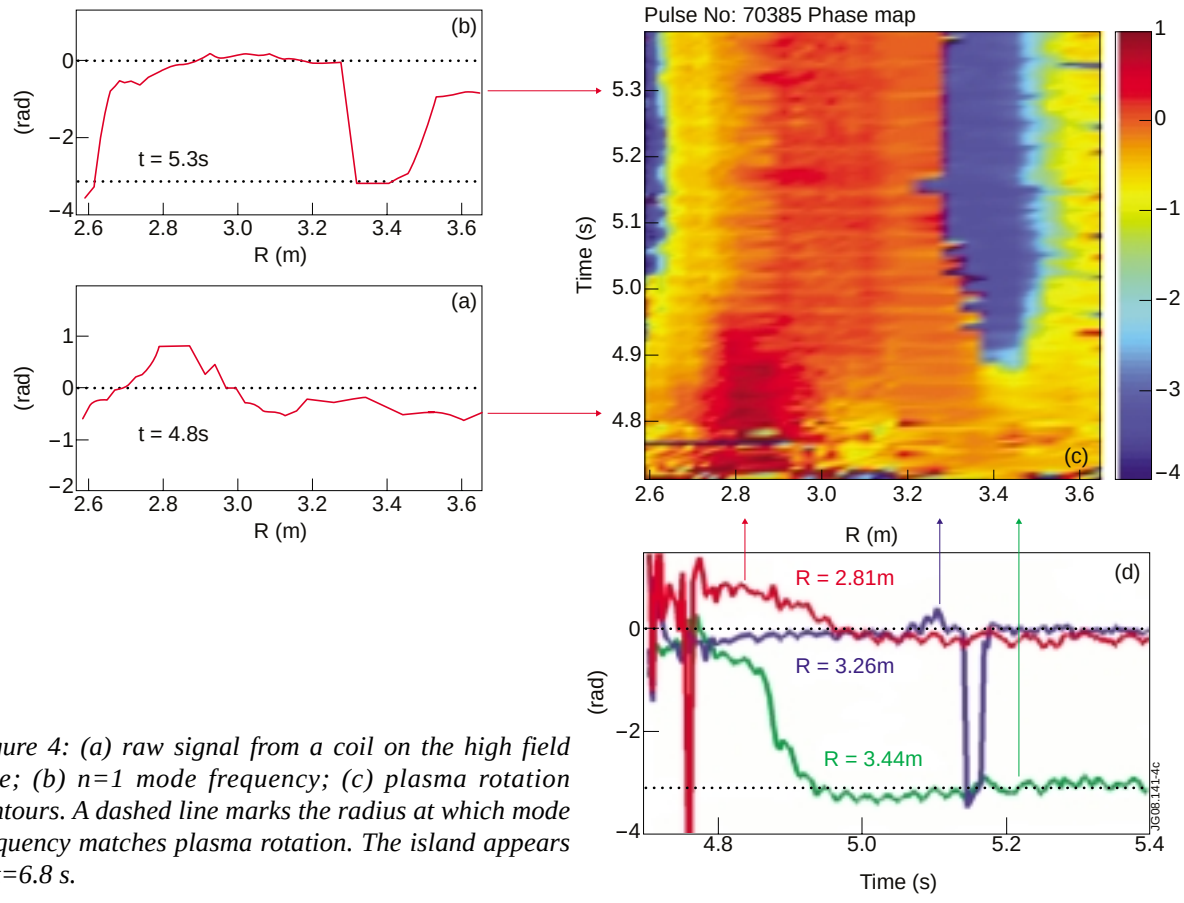

Figure 4: (a) raw signal from a coil on the high field side; (b) n=1 mode frequency; (c) plasma rotation contours. A dashed line marks the radius at which mode frequency matches plasma rotation. The island appears at t=6.8 s.